Magnetic, structural, and Raman characterization of RBa$_2$Cu$_2$NbO$_8$(R = Pr, La, or Nd)

M. Bennahmias and J. C. O'Brien
Lawrence Livermore National Laboratory, Livermore, California 94550

H. B. Radousky
Lawrence Livermore National Laboratory, Livermore, California 94550
and Department of Physics, University of California, Davis, Davis, California 95616

T. J. Goodwin, P. Klavins, J. M. Link, C. A. Smith, and R. N. Shelton
Department of Physics, University of California, Davis, Davis, California 95616
(Received 3 June 1992)

PrBa$_2$Cu$_2$NbO$_8$ (PrBCNO) is an insulator analogous to the PrBa$_2$Cu$_3$O$_7$ system having a similar structure but with NbO$_2$ planes replacing the CuO chains. Single-phase polycrystalline samples of RBCNO have been synthesized with R = La, Pr, or Nd. These materials were characterized using magnetization, thermal gravimetric analysis in different atmospheres, x-ray diffraction, and Raman spectroscopy. The PrBCNO samples show a signature in the magnetization of a magnetic ordering at 12 K. No such magnetic phase transition is observed down to 2 K in NdBa$_2$Cu$_2$NbO$_8$.

INTRODUCTION

It is well known that a variety of high-temperature superconducting RBa$_2$Cu$_3$O$_7$ (RBCO, R is any rare-earth element except Ce, Pr, and Tb) compounds can be readily synthesized with T_c near 90 K. The rare-earth elements Ce and Tb do not form the RBCO phase using standard solid-state reaction techniques and Pr forms an isostructural insulating analog.[1] These cuprates all possess the YBCO crystallographic structure, which consists of an orthorhombic oxygen-deficient triple layer of perovskite-type cells, stacked along the c axis. The Cu in these materials resides in two distinct sites; namely, the square planar fourfold coordination Cu(1) site within the one-dimensional Cu-O chains, located between successive Ba layers, and in the tetragonal pyramidal fivefold coordination Cu(2) site within the CuO$_2$ sheets, sandwiched between adjacent Ba and rare-earth ion planes. It is widely accepted that the electronic characteristics of the CuO$_2$ planes, specifically the dominant Cu 3d to O 2p hybridization effects, are essential to the dynamics of high-T_c superconductivity in these RBCO phases while the Cu-O chains provide the crucial free carrier reservoirs for charge transport. Electronic transport properties of PrBCO using the standard four-probe technique have found the PrBCO phase to be a relatively "weak" electrical insulator which has been attributed to the effects of variable range hopping of conduction electrons along the Cu-O chains. Efforts aimed at developing a better class of electrical insulators to serve as lattice matched buffer layers in RBCO multilayer device structures have centered on chemical substitution of NbO$_2$ and TaO$_2$ layers in place of the Cu-O chains.[2,3] Additional interest has been generated by the suggestion that these RBCNO materials might become superconducting if they could be properly doped[4] and the possibility of using them as low dielectric substrates in microwave stripline applications.[5]

LaBa$_2$Cu$_2$$MO_8$ (LaBCMO, M = Nb, Ta) was studied by several groups.[6-8] Ichinose *et al.*[9] successfully synthesized RBa$_2$Cu$_2$$MO_8$ (RBCMO, R = Pr and La, M = Nb and Ta). Rietveld analysis of powder x-ray diffraction[6,9] as well as neutron diffraction[7,8] on the RBCMO materials have determined the structure to be a tetragonal YBCO-like structure with the Cu-O chains replaced by MO$_2$ planes. Determination of the lattice parameters for these RBCMO phases has demonstrated the lattice mismatch between the parent RBCO orthorhombic phase to be $<2\%$ within the CuO$_2$ planes and along the c axis. Preliminary studies on the room-temperature electrical transport properties of PrBCMO using the standard four-probe technique have indicated these insulators exhibit three to five orders of magnitude improvement over the parent compound PrBCO in terms of bulk electrical resistivity.[2]

In this paper we report the preparation, structure, oxygen content, reduction chemistry, magnetic properties, and Raman spectra of three of the members of the Nb metal-doped family of electrical insulators RBa$_2$Cu$_2$NbO$_8$ (RBCNO, R = Pr, La, and Nd). The discussion covers the issue of observing superconductivity in these materials with appropriate doping, and draws some analogies between the appearance of a large antiferromagnetic ordering transition (T_N = 12 K) in the PrBCNO insulator with that found in the previously well-characterized PrBCO insulator ($T_N \approx 17$ K).

EXPERIMENT DETAILS

The polycrystalline samples PrBCNO, LaBCNO, and NdBCNO used in this study were synthesized through conventional solid-state reaction methods. Stoichiometric amounts of high-purity (99.99% or better)

Pr_6O_{11}, $BaCO_3$, CuO, Nb_2O_5, La_2O_3, and Nd_2O_3 dried powders were appropriately mixed, ground, and reacted in air at 1000° C for 12 hours. Each calcined mixture was then reground and the firing process repeated. Subsequently, the powders were pressed into pellets, sintered in air at 1025 °C for an additional 24 hours, and then allowed to furnace cool back down to room temperature.

Powder x-ray-diffraction data were taken at room temperature with a Siemens D-500 diffractometer using Cu $K\alpha$ radiation. The 2θ measurements were obtained over the angular range of 10° to 120° with a step size of 0.02° and a scan time of 8 seconds per step. Structure parameters were determined by Reitveld[10] analysis of the x-ray-diffraction patterns using the GSAS (Ref. 11) software package. Magnetic susceptibility data were obtained with a quantum design superconducting quantum interference device magnetometer over the temperature range of 2 to 300 K in a magnetic field of 5000 Oe. Thermal gravimetric analysis (TGA) measurements were performed using a DuPont 951 thermal analysis system in three different atmospheres: forming gas (6% H_2/94% N_2), nitrogen, and oxygen. A typical TGA scan involved flowing the reducing gas through the sample chamber at a flow rate of 50 cc/min while at the same time ramping up the temperature from 25 to 1050 °C at 5 °C/min. Raman spectra were obtained at room temperature, in air, using a standard Raman spectroscopy setup which included a Spex triplemate spectrometer and a liquid-nitrogen-cooled charge coupled device (CCD) array, with the integration time being ten minutes per spectra. The data were collected in a backscattering geometry using the 514-nm line on an argon-ion laser as the excitation source, with an approximate laser intensity of 1 W/cm^2.

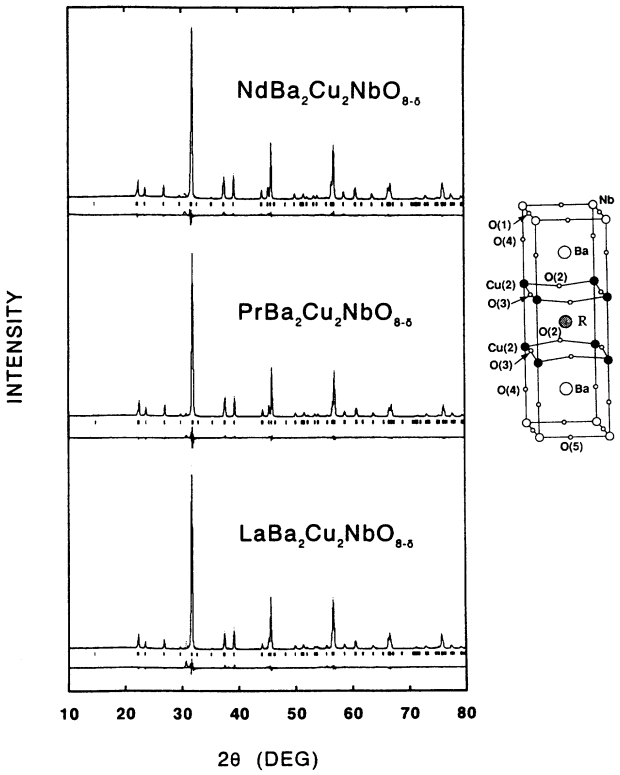

FIG. 1. Room-temperature x-ray powder diffraction spectra using Cu $K\alpha$ radiation and Reitveld analysis of PrBCNO, LaBCNO, and NdBCNO. The residual error between the x-ray-diffraction pattern generated from the Reitveld analysis and the observed powder x-ray-diffraction data is also shown. The inset depicts the tetragonal perovskite crystallographic structure for these materials confirmed by Reitveld analysis.

STRUCTURAL CHARACTERIZATION

The results of the powder x-ray-diffraction measurements and Reitveld analysis on the PrBCNO, LaBCNO, and NdBCNO compounds are presented in Fig. 1 as a function of twice the Bragg scattering angle. The Nd-, Pr-, and La-based insulators all have nearly identical x-ray-diffraction spectra, with small shifts in the line positions due to the different lattice constants. Table I lists the corresponding lattice constants as determined by a standard least-squares-fit technique to the x-ray-diffraction peaks for PrBCNO, LaBCNO, and NdBCNO. The values in Table I indicate that the lattice constants have increased due to the Nb substitution into the Cu(1) sites, when compared to the corresponding *R*BCO parent material.

TABLE I. Lattice constants for *R*BCNO and *R*BCO (*R* = Pr, La, and Nd).

Compound	*a* (nm)	*b* (nm)	*c* (nm)	Volume (nm^3)
PrBCNO	0.3954	0.3954	1.1986	0.187 39
PrBCO[a]	0.3878	0.3913	1.1719	0.178 53
NdBCNO	0.3948	0.3948	1.1976	0.186 66
NdBCO[b]	0.3977	0.3921	1.1762	0.178 72
LaBCNO	0.3971	0.3971	1.2002	0.189 26
LaBCO[c]	0.3893	0.3938	1.1818	0.181 18

[a]Data taken from Neumeier *et al.* (Ref. 12).
[b]Data taken from Schneemeyer *et al.* (Ref. 13).
[c]Data taken from Ichinose *et al.* (Ref. 9).

Reitveld analysis of the x-ray-diffraction data confirmed the structure of all three *R*BCNO compounds to be an oxygen deficient, tetragonal YBCO-like structure, with the Cu-O chains replaced by NbO_2 planes. The *R*BCNO structure is illustrated pictorially in the inset of Fig. 1. All three compounds were refined to a *P4/mmm* space group. The goodness-of-fit values for LaBCNO, PrBCNO, and NdBCNO were 4.48%, 2.89%, and 2.83%, respectively. The refined structural parameters for LaBCNO and PrBCNO were identical to those previously reported by Ichinose.[9] The results of the structural parameter refinement of the NdBCNO compound, previously unreported, are presented in Table II.

Attempts to synthesize GdBCNO and YBCNO analogs proved unsuccessful. Instead these rare-earth elements (*R*) formed multiphase materials comprised of a single-cell pseudocubic perovskite structure RBa_2NbO_6,[14] an R_2BaCuO_5 phase, and traces of unreacted CuO and R_2O_3 oxides. This finding suggests there exists an ionic size effect, with Gd and Y being too small to successfully form the *R*BCNO phase. Preliminary attempts to form

TABLE II. Structural parameters for NdBCNO determined from Reitveld analysis ($Rwp = 0.082$, $Rp = 0.061$, $R = 2.83\%$). The B structural parameters are a measure of the thermal motion of the constituent atoms about their equilibrium position, centered at x, y, and z.

Atom	x	y	z	B (Å^2)
Nd	0.5	0.5	0.5	0.12
Ba	0.5	0.5	0.195 73	0.15
Nb	0.0	0.0	0.0	0.13
Cu	0.0	0.0	0.358 15	0.16
O(1)	0.0	0.0	0.168 35	0.22
O(2)	0.5	0.0	0.0	0.37
O(3)	0.0	0.5	0.374 35	0.01

the RBCNO structure with Eu or Sm have also been unsuccessful. Partial substitution of the Nb for Cu in $R\mathrm{Ba_2Cu_{3-x}Nb_xO_8}$ results in a single-phase material only for $x = 1$.

In order to properly evaluate the purity of the RBCNO materials we synthesized, it was necessary to determine the peak detection sensitivity of the x-ray diffractometer to the possible presence of small amounts of secondary rare-earth-based phases that may have inadvertently formed, such as the orthorhombic magnetic perovskite $\mathrm{PrBaO_3}$(PrBO) and $\mathrm{PrBa_2NbO_6}$ (PrBNO) in the case of PrBCNO. To accomplish this, controlled amounts of PrBO, chosen because of similar magnetic ordering features of the PrBCNO, were thoroughly mixed together with PrBCNO and subsequently examined in the x-ray diffractometer to assess at what level the PrBO "impurity" peaks could be observed in the date. Three glass x-ray slides were prepared with PrBCNO to PrBO weight percentage ratios of 99:1, 97:3, and 95:5. The results, including the x-ray spectra from PrBCNO for comparison, are shown in Fig. 2 as a function of twice the Bragg scattering angle, with the stronger of the x-ray-scattering peaks of the PrBO lines identified. The strongest of these x-ray-scattering peaks has been established as originating from a collective superposition of three very close crystallographic planes in the PrBO material. As expected, the strength of the impurity lines increased with increased PrBO content. The PrBO x-ray-diffraction peaks are readily observable even when a concentration of 1% PrBO is added. The x-ray spectra for $\mathrm{PrBa_2NbO_6}$, as shown in Fig. 3 as a function of twice the Bragg scattering angle, also clearly indicates that similar intense x-ray peak features would provide strong identification markers that would help improve the capability for detection of this phase in the powder x-ray-diffraction data if it were present. These results suggest that the synthesized samples appear to be single phase to better than 1% with respect to potential RBO and RBNO impurities. It is estimated that the materials are single phase with respect to other nonprimary and secondary phases such as $\mathrm{BaCuO_2}$ to better than 3%.

The weight loss profile of the PrBCNO, LaBCNO, and NdBCNO materials as a function of temperature, in a forming gas (6% $\mathrm{H_2}$/94% $\mathrm{N_2}$) reduction atmosphere, is presented in Fig. 4. Oxygen loss for both the Pr and La phases was observed to occur starting around 300 °C with mass loss saturating in the Pr system by 420 °C and in the La system by 470 °C. The Nd compound was seen to be slightly less reactive to the forming gas reducer as mass loss did not start until 430 °C with mass loss saturation occurring by 480 °C. No further mass loss was observed for any of the RBCNO systems out to 1050 °C. The reduction reaction for the RBCNO members by $\mathrm{H_2}$ has been empirically established via identification of the reduction products by x-ray diffraction as

$$R\mathrm{Ba_2Cu_2NbO_{8-\delta}} + (2-\delta)\mathrm{H_2} \rightarrow R\mathrm{Ba_2NbO_6} + 2\mathrm{Cu} + (2-\delta)\mathrm{H_2O}\ .$$

Attempts at trying to thermodynamically reverse this reduction reaction starting from the reduction products and trying to reintroduce oxygen in order to recover the original material proved unsuccessful. The lack of total

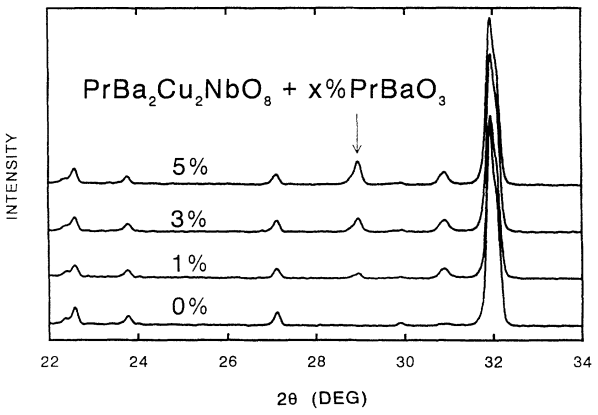

FIG. 2. Room-temperature x-ray powder diffraction spectra taken of PrBCNO and PrBO mixtures in weight percentage ratios of 100:0, 99:1, 97:3, and 95:5. The arrow indicates the strong scattering peaks from PrBO used to determine the detection sensitivity of this magnetic perovskite from the x-ray data.

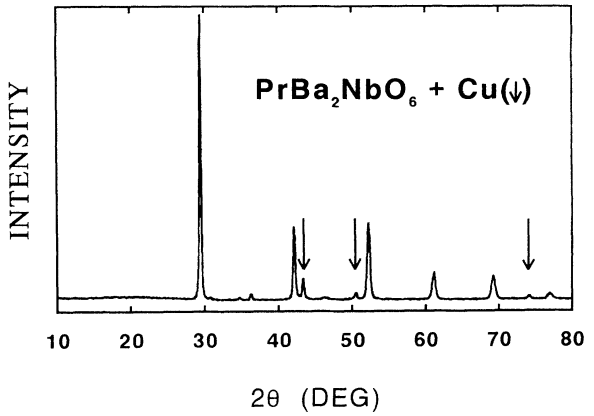

FIG. 3. Room-temperature x-ray powder diffraction data for PrBCNO after being reduced in forming gas (6% $\mathrm{H_2}$/94% $\mathrm{N_2}$) showing the presence of PrBNO and Cu lines.

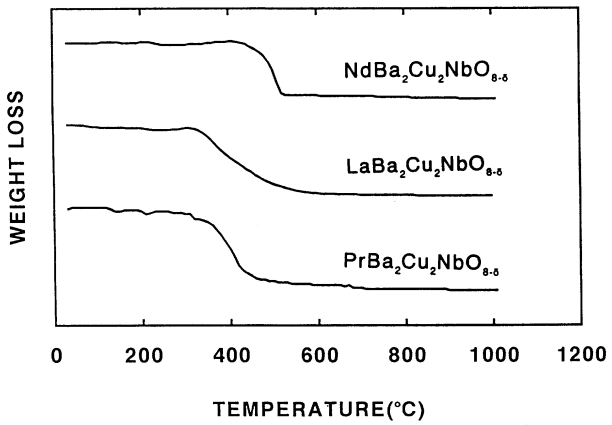

FIG. 4. Thermogravimetric traces in forming gas taken for PrBCNO, LaBCNO, and NdBCNO samples over the temperature range 25 to 1050° C.

decomposition observed in these thermogravimetric traces, as commonly seen in the reduction chemistry of the *R*BCO materials,[15] suggests that the *R*BNO compounds have better thermodynamic stability due to the presence of Nb. From a knowledge of the final reduction products, in the decomposition reaction, the oxygen contents for the La, Pr, and Nd materials, determined by estimating the value of δ, were 7.92±.02, 8.02±.02, and 7.93±.02, respectively.

The presence of Nb was observed to dramatically change the reduction chemistry in the *R*BCNO analogs, relative to what has been found for the parent *R*BCO systems. Figure 5 illustrates this point, where thermogravimetric traces for decomposition of PrBCNO, heated in forming gas, nitrogen, and oxygen, are shown for comparison. In sharp contrast to the weight loss of the PrBCNO phase in forming gas, the oxygen trace shows no appreciable weight loss out to 1050 °C, while in nitrogen the reduction is not initiated until the temperature is

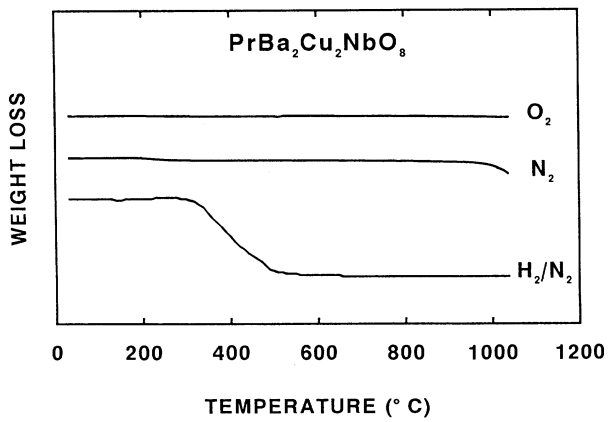

FIG. 5. Thermogravimetric traces comparing the effects of exposure to the different atmospheres of forming gas, nitrogen, and oxygen on the PrBCNO compound.

near 1000 °C. Interestingly, the x-ray-diffraction pattern taken on the sample of the PrBCNO material after reduction in nitrogen indicated that while the PrBNO phase was still present, the Cu was reduced as the Cu_2O phase and not as a pure metal.

MAGNETIZATION

The magnetic susceptibilities of the Pr-, Nd-, and La-based *R*BCNO samples were examined up to 300 K. The results are shown in Fig. 6 with the magnetic susceptibilities plotted as a function of temperature. The magnetic susceptibilities were all positive and could be fitted by a Curie-Weiss dependence of the form $\chi=\chi_0+C/(T-\theta)$, where χ_0 is the temperature-independent susceptibility, C is the Curie constant, and θ is related to the ordering temperature. From the Curie constant, the value for the effective magnetic moment μ_{eff} was determined from the relationship $C=N\mu_{\text{eff}}^2/3K_B$, where N is the number of magnetic ions per unit volume and K_B is the Boltzmann constant. Table III provides the values of the temperature range used for the data fits, χ_0, C, θ, and μ_{eff} for the paramagnetic susceptibility profiles of the PrBCNO, LaBCNO, and NdBCNO samples.

In addition PrBCNO shows a distinct signature of a magnetic transition occurring at ~12 K while there is no evidence of such a magnetic ordering in NdBCNO or LaBCNO from the magnetization data down to 1.85 K. Preliminary neutron-scattering data indicate that the NdBCNO material orders at 1.7 K.[16] The inset of Fig. 6 provides an expanded view of the magnetization for PrBCNO from 2 to 25 K. The shape of the PrBCNO ordering is similar to that previously observed in PrBCO

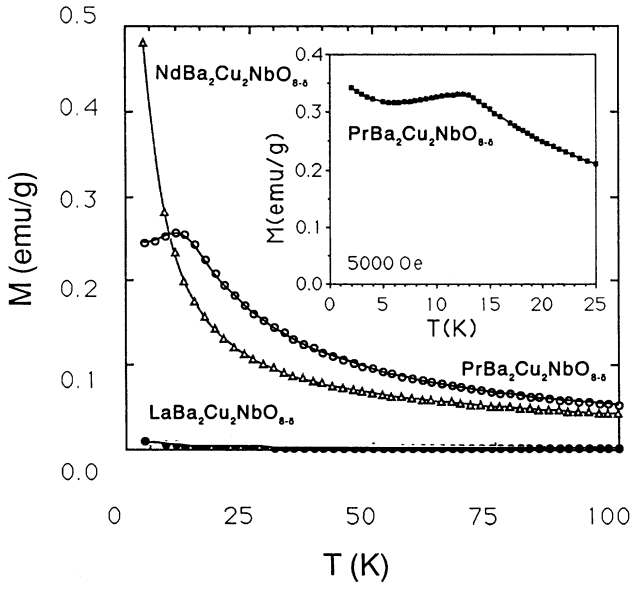

FIG. 6. Magnetic susceptibility data taken on the PrBCNO, LaBCNO, and NdBCNO materials in the field of 5000 Oe over the temperature range 4 to 300 K. The inset shows an expanded view of the ordering of the PrBCNO magnetic phase transition down to 2 K.

TABLE III. Magnetic susceptibility fit parameters for *R*BCNO (*R* = Pr, La, and Nd).

Compound	Fit range (K)	χ_0	C (K)	θ (K)	μ_{eff} μ_B
PrBCNO	20–300	1.12×10^{-6}	1.29×10^{-3}	−6.57	2.81
NdBCNO	2–300	6.04×10^{-6}	7.04×10^{-4}	−1.16	2.07
LaBCNO	2–300	1.68×10^{-7}	1.40×10^{-5}	−4.29	0.30

(Ref. 17) and CmBCO (Ref. 18). In order to eliminate the possibility that the magnetic ordering that was observed might have been due to the presence of a small amount of the magnetic perovskite $PrBaO_3$, a sample of $PrBaO_3$ was synthesized and magnetization and x-ray data were subsequently taken. $PrBaO_3$ exhibits a strong magnetic transition contribution riding on a relatively weak Curie-Weiss curve at a similar ordering temperature of ~11.7 K.[19,20] The results show that while the two magnetic phase orderings have, in fact, similar T_N values, the shapes of these profiles are distinctly different. Using the value from the x-ray results, the possible presence of less than 1 wt. % of $PrBaO_3$ would have a negligible effect on the susceptibility of PrBCNO.

RAMAN SPECTROSCOPY

The results of the Raman experiments on the Pr-, Nd-, and La-based phases are shown in Fig. 7. The lines in these Raman spectra are assumed to have similar assignments to those lines in the PrBCO Raman spectrum.[1] The out-of-phase phonon mode of the O(1) and O(2) oxygen sites in the Cu(2)-O_2 planes is seen in the data at ~301 cm^{-1} for the Pr and La structures and at ~317 cm^{-1} for the Nd structure. The inset in Fig. 7 plots this phonon mode as a function of ionic radius with the corresponding values for the undoped parent *R*BCO compounds shown for comparison.[21] Similarly, the in-phase vibrational mode of the oxygens in the Cu(2)-O_2 planes can be seen to appear at ~438 cm^{-1}, where one would expect to observe a line for that particular mode in the corresponding PrBCO data. We also see phonon vibrational modes that are typically associated with the Ba and Cu(2) constituents, at ~148 and ~122 cm^{-1}, respectively, in the PrBCO materials. There are also additional Raman lines that are present down below 120 cm^{-1}, not observed in conventional *R*BCO spectra; these may be due to the presence of Nb. In sharp contrast however, we do not see the prominent 500-cm^{-1} peak, associated with the Cu(1)-O(4)-Cu(2) vibration, which is generally the strongest Raman-active mode observed in polycrystalline *R*BCO materials. The exact reason for the absence of this feature is not known at this time. It is interesting to note that this is the vibration which would be most affected by the presence of the Nb, now being a Nb-O(4)-Cu(2) vibration. The 687-cm^{-1} line has not been assigned but the possibility of this mode originating from an impurity has not been ruled out. $BaCuO_2$ in bulk materials has been shown previously to be a very strong Raman scatterer in this wave-number region while remaining virtually undetectable in the x-ray-diffraction data.[21] Another explaination might be that the line seen at ~687 cm^{-1} potentially represents a hardening of the 500-cm^{-1} line due to the Nb localized substitution into the Cu(1) sites, or might be due to an oxygen defect mode. Polarization studies on single crystals of these materials are needed to determine the exact symmetries and identification of the various lines and the potential influence grain boundaries might have on the Raman signals from the polycrystalline samples.

Some other interesting features that were observed in the Raman data were the presence of a 205-cm^{-1} line in the NdBCNO spectra that is believed to originate from the oxygen defect mode. The NdBCNO material also exhibited a larger shift in the frequency of the 316-cm^{-1}

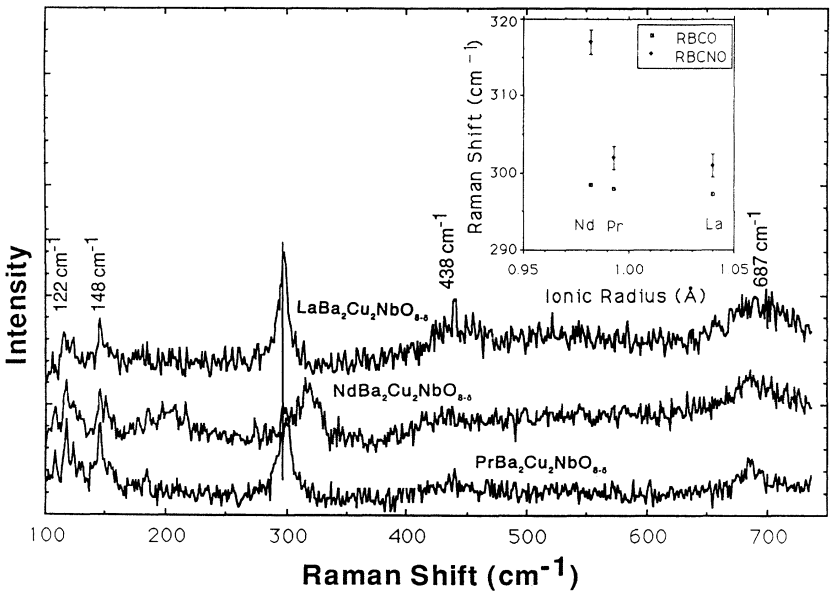

FIG. 7. Room-temperature Raman spectra in air for the PrBCNO, LaBCNO, and NdBCNO materials. The solid line is used to illustrate the difference in the Raman shift observed for the asymmetric vibrational mode in the NbBCNO compound at 317 cm^{-1} and that observed for the PrBCNO and LaBCNO compounds at 301 cm^{-1}. The inset plots the location of the asymmetric vibration mode as a function of ionic size. The values for the parent material *R*BCO Raman shifts shown in the inset have been taken from Ref. 1.

mode than did the other two materials. Overall, the shift in Raman lines for the LaBCNO material in comparison to the PrBCNO material was not as large as the shift observed between LaBCO and PrBCO.

DISCUSSION

As in the case of the *R*BCO materials, the *R*BCNO analog with Pr once again appears to be the most interesting phase because of the large magnetic ordering transition that occurs at $T_N = 12$ K. This is reminiscent of the situation in the *R*BCO materials where Pr has an ordering at 17 K, while the next highest ordering is for GdBCO at 2.2 K. For the PrBCO case, the magnetic transition has been ascribed to an antiferromagnetic ordering of the Pr sublattice.[22]

While the valence state of the Pr ion in PrBCO has been a subject of some controversy,[1] the valence state of the Pr ion in PrBCNO is unambiguously +3. This is apparent from simple valence counting arguments, the volume with respect to the other *R*BCNO materials,[23] and the application of the bond valence sum technique,[24] where the valence for the Pr ion in the PrBCNO structure comes out to be approximately +3.

The $2.8\mu_B$ measured from the data in Fig. 6 can be understood as coming from the Pr^{+3} valence state. The value for the Pr moment found in PrBCO has been explained by Soderholm *et al.*[25] as a reduction of the Pr^{+3} free ion moment due to the action of crystal fields. This reasoning is also consistent with the similar value of the Pr moment found in the PrBCNO analog. Since the Nb is fairly removed from the Pr, La, and Nd ions within their respective unit cells, it is reasonable to assume that the crystal fields at the Pr site should not be radically different from PrBCO, resulting in a similar effective moment for the PrBCO and PrBCNO materials.

The small moment found for LaBCNO is consistent with having no *f* electrons present, but the reduced moment of the NdBCNO is unexpected, and not understood at this time. The NdBCNO material is also anomalous with respect to the Raman shift of the out-of-phase bending mode relative to the PrBCNO and LaBCNO materials.

Mattheiss[4] has recently predicted that insulating phases such as LaBCNO could become superconductors if the proper dopant levels of carriers onto the Cu(2)-O_2 planes could be achieved. This was based on the similarity of the electronic band structure between LaBCNO and YBCO. Removing oxygen atoms in the Cu(1)-O chains effects the hole concentration of the Cu(2)-O_2 planes in YBCO, producing either a tetragonal insulating phase or an orthorhombic superconducting phase. From a structural point of view, the *R*BCNO insulating analogs provide an excellent vehicle for studying hole transport mechanisms leading to the onset of superconductivity since the Cu(2)-O_2 planes are not directly disturbed by the local Nb substitution into the Cu(1) sites, an important fact since intermixing of the transition-metal constituents would most likely preclude the occurrence of superconductivity. This allows for the possibility of partially doping in various elements in place of the trivalent rare-earth elements or Nb in order to observe the effects such substitutions have on the electronic band structure of the Cu(2)-O_2 planes. Initial attempts by Greaves and Slater[8] to increase the Cu(2) oxidation state in LaBCNO through partial chemical substitution of Ca^{2+} and Sr^{2+} for La^{3+} and Ti^{+4} for Nb^{+5} using conventional solid-state reaction techniques proved unsuccessful, suggesting the fact that the synthesis of these doped materials may be very sensitive to the preparation process.

It is interesting to try and predict whether the Pr in PrBCNO would inhibit superconductivity, even if a proper number of carriers could be doped into the CuO_2 planes. We note that in those materials with an anomalously high T_N with respect to the other rare-earth members of that series, no superconductivity is observed. The two prime examples are PrBCO ($T_N = 17$ K) and CmBCO ($T_N = 22$ K). Compounds where the T_N is consistent with the other rare-earth members, such as $Pr_{2-x}Ce_xCuO_4$, are superconducting. While the exact mechanism of suppression of T_c with Pr addition is still controversial, it has become clear that *f* electron hybridization plays a key role both in mediating the values of T_N and in allowing the superconductivity to be affected.[1] Based on this analogy, we might anticipate that LaBCNO and NdBCNO would be superconducting if properly doped, but that doping PrBCNO ($T_N = 12$ K) may not lead to superconductivity.

ACKNOWLEDGMENTS

The authors wish to thank Dr. L. Soderholm for helpful discussions. Work at Lawrence Livermore National Laboratory and University of California, Davis was performed under the auspices of the U.S. Department of Energy under Contract No. W-7405-ENG-48. Part of the work done at University of California, Davis was supported by the National Science Foundation under Grant No. DMR-90-21029.

[1] See the review by H. B. Radousky, J. Mater. Res. **7**, 1917 (1992) and references therein.

[2] C. T. Rogers, A. Inam, R. Ramesh, J. M. Tarascon, K. Remschnig, B. J. Wilkins, and D. L. Hart, IEEE Trans. Magn. **27**, 1600 (1991).

[3] H. Izumi, K. Ohata, T. Sawada, S. Kawamoto, T. Wada, Y. Yaegashi, H. Yamauchi, T. Morishita, and S. Tanaka, Physica C **185-189**, 2047 (1991).

[4] L. Mattheiss, Phys. Rev. B **45**, 2442 (1992).

[5] M. Bennahmias, H. B. Radousky, D. Miller, V. R. Latorre, P. Klavins, and R. N. Shelton (private communication).

[6] N. Murayama, E. Sudo, K. Kani, A. Tsuzuki, S. Kawakami, M. Awano, and Y. Torii, Jpn. J. Appl. Phys. **27**, L1623 (1988).

[7]M.-J. Rey, Ph. Dehaudt, J. Joubert, and A. W. Hewat, Physica C **167**, 162 (1990).
[8]C. Greaves and P. R. Slater, Physica C **161**, 245 (1989).
[9]A. Ichinose, T. Wada, H. Yamauchi, and S. Tanaka, J. Ceram. Soc. Jpn. Inter. Ed. **97**, 1053 (1989).
[10]H. M. Reitveld, Acta. Crystallog. **22**, 151 (1967).
[11]A. C. Larson and R. B. Von Dreele (unpublished).
[12]J. J. Neumeier, T. Bjornholm, M. B. Maple, J. J. Rhyne, and J. A. Gotaas, Physica C **166**, 191 (1990).
[13]J. V. Scheemeyer, S. M. Zahorak, R. B. van Dover, and T. Siegrist, Mat. Res. Bull. **22**, 1467 (1987).
[14]V. S. Filip'ev and E. G. Fesenko, Kristallografiya **10**, 626 (1965) [Sov. Phys. Crystallogr. **10**, 532 (1966)].
[15]X. P. Jiang, J. S. Zhang, J. G. Huang, J. Jiang, G. dW. Qiao, Z. Q. Hu, and C. X. Shi, Mater. Lett. **7**, 250 (1988).
[16]J. W. Lynn (private communication).
[17]A. Kebede, C. S. Jee, J. Schwegler, J. E. Crow, T. Mihalisin, G. H. Myer, R. E. Solomon, P. Schlottmann, M. V. Kuric, S. H. Bloom, and R. P. Guertin, Phys. Rev. B **40**, 4453 (1989).
[18]L. Soderholm, G. L. Goodman, U. Welp, C. W. Williams, and J. Bolender, Physica C **161**, 252 (1989).
[19]J. B. Bulman, M. V. Kuric, R. P. Guertin, S. Foner, E. F. McNiff, Jr., G. Cao, J. O'Riely, J. E. Crow, P. P. Wise, and T. Yuen, J. Appl. Phys. **69**, 4874 (1991).
[20]M. Bickel, G. L. Goodman, L. Soderholm, and B. Kanellakopulos, J. Solid State Chem. **76**, 178 (1988).
[21]H. J. Rosen, R. M. McFarlane, E. M. Engler, V. Y. Lee, and R. D. Jacowitz, Phys. Rev. B **38**, 2460 (1988).
[22]W-H. Li, J. W. Lynn, S. Skanthakumar, T. W. Clinton, A. Kebede, C.-S. Jee, J. E. Crow, and T. Mihalisin, Phys. Rev. B **40**, 5300 (1989).
[23]H. B. Radousky, J. C. O'brien, M. Bennahmias, P. Klavins, C. A. Smith, J. M. Link, T. Goodwin, and R. N. Shelton, in *Layered Superconductors: fabrication, properties, and applications,* edited by D. T. Shaw, C. C. Tsuei, T. R. Schneider, and V. Shidhara, MRS Symposia S Proceedings No. 275 (Materials Research Society, Pittsburgh, in press), pp. 113–118.
[24]L. Jansen and R. Block, Physica C **181**, 149 (1991).
[25]L. Soderholm, G. L. Goodman, C.-K. Loong, and B. D. Dabrowski, Phys. Rev. B **43**, 7923 (1991).

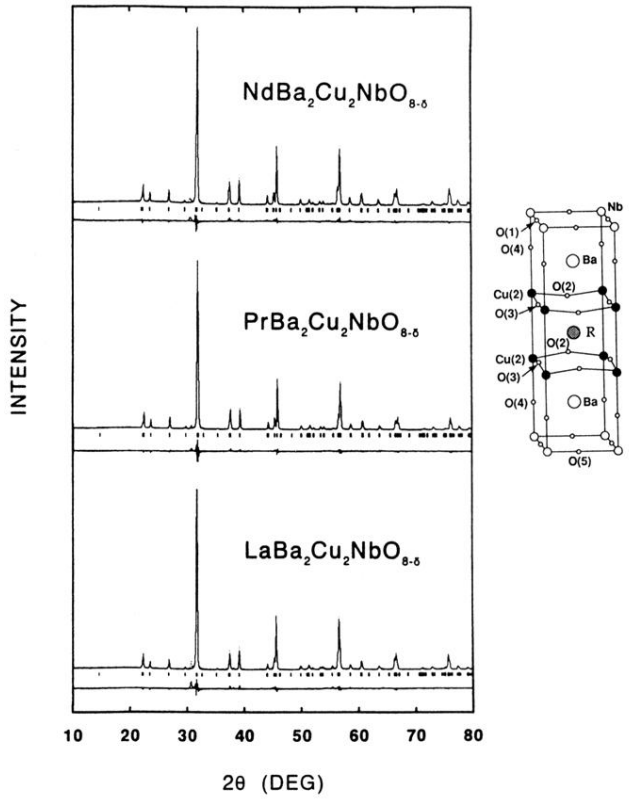

FIG. 1. Room-temperature x-ray powder diffraction spectra using Cu $K\alpha$ radiation and Reitveld analysis of PrBCNO, LaBCNO, and NdBCNO. The residual error between the x-ray-diffraction pattern generated from the Reitveld analysis and the observed powder x-ray-diffraction data is also shown. The inset depicts the tetragonal perovskite crystallographic structure for these materials confirmed by Reitveld analysis.